ELSEVIER

Polymer 43 (2002) 5473–5481

polymer

www.elsevier.com/locate/polymer

Templating of inorganic nanoparticles by PAMAM/PEG dendrimer–star polymers

Ronald C. Hedden*, Barry J. Bauer, A. Paul Smith, Franziska Gröhn, Eric Amis

National Institute of Standards and Technology, Gaithersburg, MD 20899, USA

Received 15 April 2002; received in revised form 25 June 2002; accepted 26 June 2002

Abstract

Poly(amidoamine) (PAMAM) dendrimers with amine endgroups (PAMAM–NH_2) are converted to starlike copolymers by grafting of monofunctional poly(ethylene glycol) (PEG) 'arms' onto the dendrimer endgroups. Generation 4, 7, and 10 dendrimers are converted to 60-arm, 235-arm, and 750-arm PAMAM/PEG stars, respectively. The dendrimer–stars are studied as polymer templates for stabilization of gold and cadmium sulfide nanoparticles of 1–6 nm diameter. PAMAM/PEG star templating reactions are studied by aqueous gel permeation chromatography, ultraviolet–visible absorption spectroscopy, fluorescence spectroscopy, and transmission electron microscopy. PAMAM/PEG stars effectively control nanoparticle size in the same way as PAMAM–NH_2 dendrimers. However, PAMAM/PEG stars are miscible with a wider range of solvents and with selected polymers (e.g. polymethyl methacrylate). Potential applications of dendrimer–inorganic hybrid materials (solution-phase catalysis, additives for polymer blends) could benefit from the versatile solubility of PAMAM/PEG stars. © 2002 Published by Elsevier Science Ltd.

Keywords: Star polymer; Dendrimer; Nanoparticle

1. Introduction

Poly(amidoamine) (PAMAM) dendrimers are highly branched macromolecules prepared by alternating the addition of methyl acrylate and ethylene diamine monomers to a multi-functional core, resulting in a layered, treelike structure [1]. PAMAM dendrimers have been extensively studied as hosts for encapsulated nanometer-sized metal or semiconductor particles [2–21]. In solution, selected transition metal salts (including Au^{3+}, Pd^{2+}, Pt^{2+}, Cu^{2+}, Ni^{2+}, and Ru^{3+} salts) segregate inside PAMAM dendrimers. Segregation is driven either by electrostatic interactions or coordination with the amine and amide groups in the dendrimer repeat units [2–5]. A subsequent chemical reaction converting the segregated metal salt to an insoluble metal or semiconductor can result in stable dendrimer-encapsulated nanoparticles under appropriate reaction conditions.

Studies of PAMAM–inorganic nanocomposites are motivated by a desire to understand the templating of inorganic nanoparticles by polymers [10,19]. ('Templating' implies that the polymer exerts some degree of control over the nanoparticle size distribution. 'Stabilizing' refers in general to any mechanism by which a stable polymer–inorganic nanocomposite is formed.) Dendrimers are chosen as a model templating system because they are monodisperse and structurally well-defined. Dendrimer–inorganic nanocomposites have also generated interest due to potential applications in catalysis [2,21–25]. Applications depend on achieving control over nanocomposite properties, motivating further study of templating fundamentals.

Research on dendrimer nanotemplating aims to control the size and polydispersity of the inorganic particles while maintaining the monodisperse size of the dendrimers (i.e. avoiding aggregation and precipitation). To date, several structural variations of PAMAM dendrimers have therefore been studied as polymeric templates. The number of monomer layers in the dendrimer (called 'generation', abbreviated G1, G2, G3,…) has been identified as a key parameter affecting nanotemplating [18,19]. Another important variable is the type of dendrimer endgroups, which governs the formation of multi-dendrimer aggregates, especially for smaller dendrimers [2,10,17,19]. Current work focuses on further establishing the effects of dendrimer chemical structure on nanotemplating reactions.

This report concerns the use of dendrimer–star polymers as nanotemplates. Dendrimer–star polymers are highly

* Corresponding author. Tel.: +1-301-975-4356; fax: +1-301-975-3928.
E-mail address: ronald.hedden@nist.gov (R.C. Hedden).

0032-3861/01/$ - see front matter © 2002 Published by Elsevier Science Ltd.
PII: S0032-3861(02)00428-7

branched dendrimer-linear copolymers with core–shell architecture. PAMAM/PEG dendrimer–stars were prepared by grafting monofunctional linear poly(ethylene glycol) (PEG) 'arms' to PAMAM dendrimers with $-NH_2$ endgroups (PAMAM–NH_2). Templating of gold and cadmium sulfide nanoparticles by PAMAM/PEG stars was then examined. By isolating the individual dendrimers in a shell of PEG chains, we hoped to simplify templating mechanisms by discouraging the formation of multi-dendrimer clusters. We also studied the effects of the grafted PEG chains on nanocomposite physical properties (such as solubility). This work concerns the effectiveness of PAMAM/PEG stars as nanotemplates, based on comparisons to previous reports on unmodified PAMAM dendrimers.

2. Experimental section[1]

2.1. Dendrimer–star synthesis

PAMAM/PEG stars were prepared by the reaction of *O*-[2-(vinylsulfonyl)ethyl]-*O'*-methyl-polyethylene glycol 5000 (Fluka), hereafter called 'PEG-VS', with PAMAM dendrimers [26]. The monofunctional PEG-VS arms had reported molar mass of $M_n = 5000\ g\ mol^{-1}$ and $M_w/M_n = 1.01$. The sample contained a small percentage of an inert linear PEG dimer. PAMAM Generation 4 (G4) Starburst™ dendrimers with theoretically 64 terminal amine groups were obtained from Aldrich, Inc. (10% in methanol, theoretical molecular mass 14,215 g mol^{-1}). PAMAM Generation 7 (G7) dendrimers with theoretically 512 terminal amine groups (25% in methanol, theoretical molecular mass 116,500 g mol^{-1}) and PAMAM Generation 10 (G10) dendrimers with theoretically 4096 endgroups (25% in methanol, theoretical molecular mass 934,000 g mol^{-1}) were donated by Dendritech, Inc.

PEG arms were attached to the dendrimer terminal $-NH_2$ groups via Michael addition in methanol (J.T. Baker). For both G4 and G7 stars, the mass fraction of combined polymers in the methanol was fixed to 20 ± 2% during the reaction. The Michael reaction proceeded at 22 ± 2 °C for 2 weeks or more before further use of the stars. (Uncertainties reported are estimates based upon the researchers' experience with the analytical equipment.)

[1] Certain commercial materials and equipment are identified in this paper in order to adequately specify the experimental procedure. In no case does such identification imply recommendation by the National Institute of Standards and Technology nor does it imply that the material or equipment is the best available for this purpose.

2.2. Star characterization by gel permeation chromatography (GPC)

Stars were characterized by GPC using Phenomenex™ GFC-P-4000 and GFC-P-3000 columns in series with 99.9% water/0.1% triethylamine (by volume) as the mobile phase. An Alltech ELSD 500 Evaporative Light Scattering Detector (hereafter called 'mass evaporative detector') and a Spectra-Physics Spectra Focus forward scanning ultraviolet detector ('UV detector') were used to monitor the column effluent. Complete separation of the stars from excess PEG-VS was achieved, permitting quantitative determination of the fractional conversion of PEG-VS to stars from the integrated intensities of the mass evaporative detector peaks. Prior to integration, mass evaporative detector intensity was corrected for its nonlinear dependence on solute concentration. Knowing the fractional conversion of PEG-VS to arms permits computation of the number-average molecular weight. The average number of arms per star molecule f was calculated as

$$f = (\text{moles PEG} - \text{VS reacted})/(\text{moles dendrimer}) \quad (1)$$

Star molecular mass was then calculated from

$$M_n = M_{\text{dendrimer}} + fM_{\text{arm}} \quad (2)$$

where $M_{\text{dendrimer}}$ is the molar mass of the dendrimer and M_{arm} is the molar mass of the PEG-VS arms. Therefore, no calibration standards were used to obtain molecular weights. The accuracy of the molecular mass determination is limited by the integration of the mass evaporative detector trace, and by the accuracy of the arm molecular mass quoted by the supplier.

2.3. Nanoparticle synthesis

CdS nanoparticles were prepared by the reaction of cadmium nitrate tetrahydrate with sodium sulfide nonahydrate in the presence of PAMAM/PEG stars. An aliquot of $(1.00 \pm 0.01) \times 10^{-2}$ mol l^{-1} $Cd(NO_3)_2{\cdot}4H_2O$ (Aldrich) in methanol was added to a solution of $(6.0 \pm 0.1) \times 10^{-6}$ mol l^{-1} PAMAM/PEG stars by a microliter syringe and was homogenized for 1–2 min by stirring. CdS particles were created by dropwise addition of methanol solution containing $(1.00 \pm 0.01) \times 10^{-2}$ mol l^{-1} $Na_2S{\cdot}9H_2O$. A 2.5 M excess of Cd^{2+} over S^{2-} was always employed.

Gold nanoparticles were prepared by the reduction of hydrogen tetrachloroaurate hydrate to Au^0 with sodium borohydride in an aqueous solution of PAMAM/PEG stars. Stars were dissolved in water at a concentration of $(3.51 \pm 0.01) \times 10^{-5}$ mol l^{-1}. An aliquot of $(1.00 \pm 0.01) \times 10^{-2}$ mol l^{-1} $HAuCl_4{\cdot}H_2O$ (Aldrich) was added to the star solution with rapid stirring and allowed to homogenize for 1–2 min. An aqueous solution containing $(1.00 \pm 0.01) \times 10^{-1}$ mol l^{-1} $NaBH_4$ (Aldrich) and $(3.00 \pm 0.03) \times 10^{-1}$ mol l^{-1} NaOH (Fisher) was prepared

in water immediately before reaction. The $NaBH_4$/NaOH solution was added in a single aliquot with rapid stirring. The mole ratio of $NaBH_4/HAuCl_4$ was 6:1 for all samples. Reactant mole ratios for individual samples are summarized in Table 1.

In both syntheses, the moles of stars (equivalently the moles of dendrimers) was calculated based on the mass of PAMAM dendrimers used in the synthesis. Uncertainty in the molar concentration of stars therefore depends on the accuracy of the dendrimer formula weight quoted by the supplier.

2.4. UV–visible spectroscopy

UV–visible absorbance spectra of samples in methanol solution were recorded on a Perkin Elmer Lambda 9 UV/vis/NIR Spectrophotometer. Star polymer concentration was the same as during synthesis. Absorbance was measured for wavelengths between 200 and 500 nm for samples in a 1 cm pathlength quartz cuvette using a light source slit width of 1 nm. The spectrum from a quartz cuvette containing methanol was subtracted from all sample spectra.

2.5. Fluorescence spectroscopy

Excitation and emission fluorescence spectra of CdS nanoparticles were measured on a SPEX Fluorolog DM3000 spectrometer with fluorescence detection in right-angle geometry. Samples were studied in quartz cuvettes with a 1 cm pathlength in methanol solution at the same concentration employed during synthesis. Spectra were corrected for background light and solvent fluorescence by subtracting the spectrum of methanol. Quinine sulfate dihydrate (NBS/NIST SRM 936A, in $(1.05 \pm 0.05) \times 10^{-2}$ mol l^{-1} aqueous $HClO_4$) was used as a standard to correct for detector response [27,28].

2.6. Transmission electron microscopy (TEM)

After waiting at least 24 h after the reduction reaction, gold-containing star samples were deposited on a Ted Pella Type B 300 mesh carbon-coated copper grid. Approximately 5 μl of aqueous Au–star solution was placed on the grid and was air-dried for several hours, followed by vacuum drying at room temperature. TEM images were obtained at 120 kV with a Phillips 400 T with magnifications up to 100,000 ×.

3. Results and discussion

3.1. PAMAM–PEG stars and nanotemplating

The reaction of the PAMAM dendrimers and monofunctional PEG-VS forms starlike molecules with many branches. Fig. 1 shows two-dimensional illustrations of the structures of a dendrimer (top) and a dendrimer–star polymer (center). (The illustrations in Fig. 1 are intended only to illustrate the connectivity of the dendrimer–star polymers and of the nanocomposites, and are not meant to represent realistic molecular conformations or relative sizes.) In solution, the star molecules are probably roughly spherical, with PEG chains forming a shell around the PAMAM dendrimer cores. When Cd^{2+} or Au^{3+} ions are introduced into a solution of the stars, the metal ions likely segregate inside the dendrimers due to favorable interactions with the dendrimer internal amides and terminal amines [2]. The templating reaction is carried out by converting the metal ions to an insoluble product (CdS or Au^0). In the absence of the dendrimer–stars, bulk CdS or Au precipitates readily from solution. In the presence of the dendrimer–stars, the precipitation results in nanometer-sized particles that can be shown to be attached to the stars (Fig. 1, bottom). The confinement of the precipitate to nanometer-size dimensions must be facilitated by favorable interaction between the dendrimer and the nanoparticle surface, deterring the flocculation of the nanoparticles. The nature of the dendrimer–nanoparticle bonding and the mechanism of particle formation have not been completely characterized to date.

3.2. GPC analysis

The conversion of PAMAM dendrimers and PEG-VS to PAMAM/PEG stars was monitored by aqueous GPC. The conversion of PEG-VS to stars reached a pseudo-equilibrium after 1–2 weeks. Fig. 2 shows GPC mass evaporative detector traces for PAMAM G4, G7, and G10 stars. The peak at shorter elution time is due to the star molecules, and the peak at longer elution time is due to excess PEG-VS. The small amount of material between the peaks was attributed to an inert PEG 'dimer' which was present in the PEG-VS starting material, the amount of which varied slightly between batches. The UV detector at 360 nm indicated no measurable signal for the excess PEG-VS and a very weak signal from the stars, which presumably arose from the dendrimer cores. The UV detector was set to 360 nm for detection of CdS or Au nanoparticles in subsequent steps.

Because the masses of dendrimer and PEG-VS in the original reaction mixture were known, the star molar mass M_n and number of arms f could be calculated from Eqs. (1) and (2). The uncertainties in f and in the fractional conversion of PEG were estimated as ±5%. The estimated uncertainty in M_n may be higher than quoted, because calculated molecular masses also depend on the molar mass of the PEG-VS arms quoted by the supplier. For the G4 stars, $M_n = (3.1 \pm 0.1) \times 10^5$ g mol^{-1} and $f = (60 \pm 3)$; for the G7 stars, $M_n = (1.3 \pm 0.1) \times 10^6$ g mol^{-1} and $f = (235 \pm 13)$; and for the G10 stars, $M_n = (4.7 \pm 0.2) \times 10^6$ g mol^{-1} and $f = (750 \pm 40)$. All samples contained a

Table 1
Nanocomposites of stars with cadmium sulfide and gold nanoparticles (uncertainties quoted in text)

CdS–star samples					
Sample name	Dendrimer generation	Endgroups (theo.)[a]	Measured number of PEG arms	CdS loading ratio[b]	Cd/S mole ratio[c]
G4 CdS 1:8	G4	64	60	1:8	2.5
G4 CdS 1:2	G4	64	60	1:2	2.5
G4 CdS 1:1	G4	64	60	1:1	2.5
G7 CdS 1:8	G7	512	235	1:8	2.5
G7 CdS 1:2	G7	512	235	1:2	2.5
G7 CdS 1:1	G7	512	235	1:1	2.5
Au–star samples					
Sample name	Dendrimer generation	Endgroups (theo.)[a]	Measured number of PEG arms	Loading ratio[d]	
G4 Au	G4	64	60	1:2	
G7 Au	G7	512	235	1:2	
G10 Au	G10	4096	750	1:2	

[a] Theoretical number of endgroups per dendrimer.
[b] Moles of CdS per mole (theoretical) dendrimer endgroups.
[c] Moles $Cd(NO_3)_2{\cdot}4H_2O$ added per mole $Na_2S{\cdot}9H_2O$.
[d] Moles of $HAuCl_4$ per mole (theoretical) dendrimer endgroups.

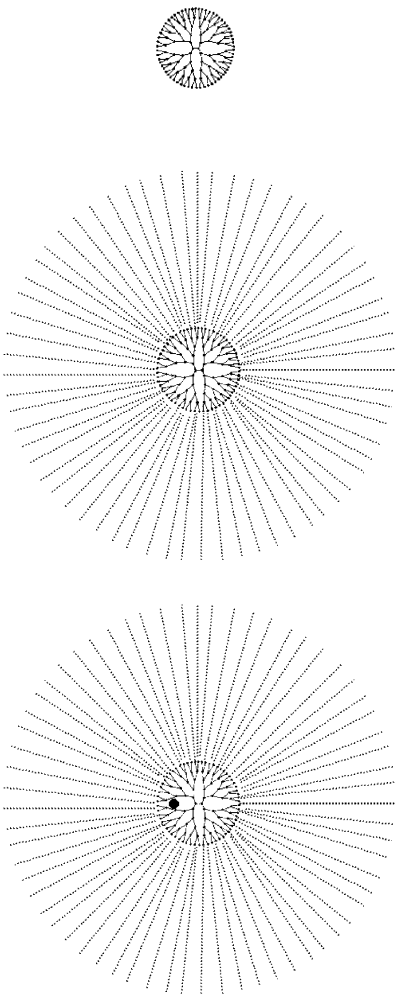

Fig. 1. Schematic drawings of the structures of a dendrimer (top), a dendrimer–star polymer (center), and a dendrimer–star polymer encapsulating a nanoparticle (bottom). See Section 3.1 for description.

certain amount of excess linear PEG. The mass fraction of excess PEG-VS and PEG dimer combined was about 0.14 for G4 stars, 0.52 for G7 stars, and 0.78 for G10 stars. Several batches of stars were prepared over the course of the study, and the amount of excess linear material varied slightly between batches. It is possible to prepare star samples with smaller amounts of leftover PEG-VS by changing the reaction stoichiometry, but it was instructive to use an excess of PEG-VS in this study.

Assuming each dendrimer amine endgroup can react once with a PEG-VS molecule, the number of PEG-VS arms that can be attached should equal the number of amine endgroups (64, 512, and 4096 for G4, G7, and G10 stars, respectively). However, the measured value of f was considerably less than the theoretical number of dendrimer endgroups for the G7 and G10 stars. The incomplete functionalization of the PAMAM dendrimers with the PEG-VS may be due to steric crowding. Another possibility is that the dendrimers, which are known to contain defects

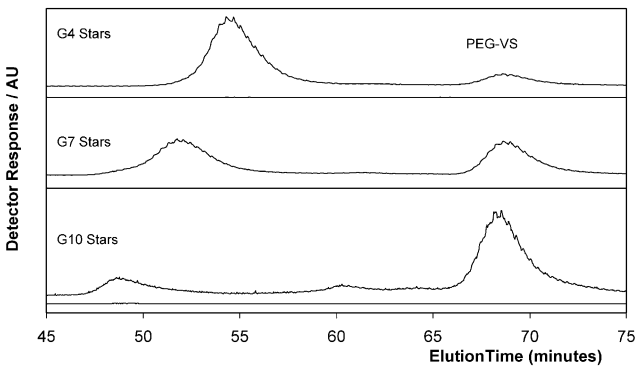

Fig. 2. Gel permeation chromatograph traces for PAMAM/PEG stars. For each sample, traces represent mass evaporative detector (top) and ultraviolet absorbance detector at 360 nm (bottom).

such as loops and missing branches [1], have fewer endgroups than the number assumed.

3.3. Dendrimer–star physical properties

The PAMAM/PEG star polymers could be isolated as a crystalline solid either with or without inorganic nanoparticles attached. Star/inorganic nanocomposites could be redissolved completely in a variety of solvents. None of the nanocomposite samples precipitated from solution during synthesis, and all nanocomposite samples passed easily through 0.2 μm Teflon filtration membranes without accumulation of material in the filter. These observations suggest there is a lack of aggregates over ~200 nm diameter in the nanocomposites.

The stars dissolve in solvents such as toluene and tetrahydrofuran at or above room temperature in addition to the good solvents for PAMAM dendrimers (water, alcohols, and dimethyl sulfoxide). In addition, PAMAM/PEG star polymers may be dispersed in other polymers to obtain optically transparent blends. Blends of 3% stars in poly(methyl methacrylate) and poly(methyl acrylate) can be prepared by casting from a good solvent [29]. Modification of PAMAM miscibility is important if dendrimer–inorganic nanocomposites are to be used for solution-phase catalysis or as additives in polymer blends. A similar approach to modifying PAMAM dendrimer solubility has been pursued by Chechik, Zhao, and Crooks [2,30]. Self-assembly of dodecanoic acid with PAMAM–NH_2 dendrimers produces inverted micelles that are soluble in hydrocarbon solvents.

3.4. Nanotemplating reaction variables: dendrimer generation and loading ratio

The dendrimer generation (number of monomer layers) is a key structural parameter affecting nanotemplating [18,19]. As PAMAM generation increases from G2 to G10, hydrodynamic diameters increase from 1 to 15 nm in good solvents [31,32], and the number of nitrogen-containing functions in the dendrimer increases exponentially. The number of metal ions that can be accommodated thus increases with dendrimer generation.

Another important variable governing nanoparticle size distributions is the metal/nitrogen 'loading ratio'. The loading ratio has traditionally been defined as the mole ratio of metal ions to the theoretical number of dendrimer endgroups [2,19]. For example, a mixture containing 32 Au^{3+} ions per G4 dendrimer (64 endgroups) is defined as having a loading ratio of 1:2. This definition is maintained in this study for consistency, and does not imply that metal ions coordinate with any specific part of the dendrimers. The maximum number of ions that a PAMAM dendrimer can accommodate has been studied previously for several metals [2]. The CdS loading ratio was varied in this study, while the Au loading ratio was held fixed at 1:2. The effects of Au loading ratio on particle size have been discussed previously for PAMAM–NH_2 dendrimers [19]. Table 1 lists loading ratios for all samples.

3.5. Nanocomposite structural analysis by aqueous GPC

After addition of CdS or Au nanoparticles, 'CdS–stars' and 'Au–stars' were analyzed by aqueous GPC. Absorptions of the nanoparticles at 360 nm were reflected in the UV detector response, whereas the polymers showed negligible UV absorption at that wavelength. The mass evaporative detector response was dominated by the mass of the polymers and was essentially unaffected by the inorganic nanoparticles, which account for a small percentage of the sample mass.

For the Au–stars with loading ratio 1:2, the UV absorbance of the nanoparticles and the mass evaporative peak of the stars had the same elution time, indicating that the nanoparticles are bound to the stars (Fig. 3). By similar logic, the excess PEG-VS did not stabilize any nanoparticles. For the G7 and G10 samples, the position and shape of the star polymer elution peak from the mass evaporative detector did not change after addition of nanoparticles. For the G4 Au–stars, a slight broadening of the mass evaporative detector trace was noted, and the UV detector peak was shifted slightly towards shorter elution time. These observations could indicate a slight increase in size of the G4 stars after addition of the gold particles. Another possibility is that the G4 Au–stars contained some small aggregates consisting of a few star molecules.

For the CdS–stars, GPC results (Fig. 4) indicated that the CdS particles were attached to the stars but not the linear PEG. When the CdS loading ratio was increased to 1:1, the position of the UV detector peak shifted to shorter elution time (larger hydrodynamic size) and its shape changed slightly. This observation might suggest that the size distribution of the stars was perturbed when the loading ratio increased past a certain limit. However, we note that no

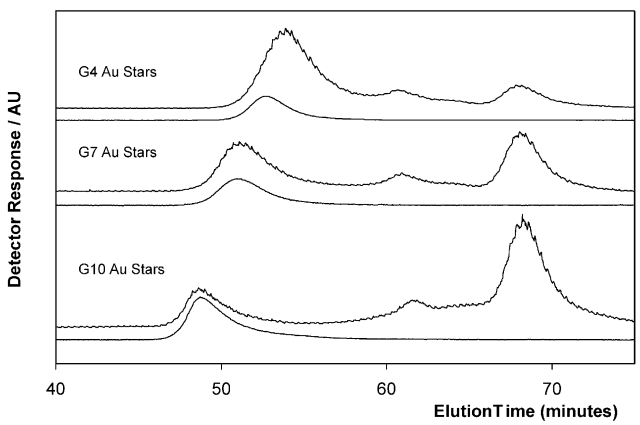

Fig. 3. Gel permeation chromatograph traces for Au–stars. Top: G4 Au–stars; middle: G7 Au–stars; bottom: G10 Au–stars. For each sample, traces represent mass evaporative detector (top) and ultraviolet absorbance detector at 360 nm (bottom).

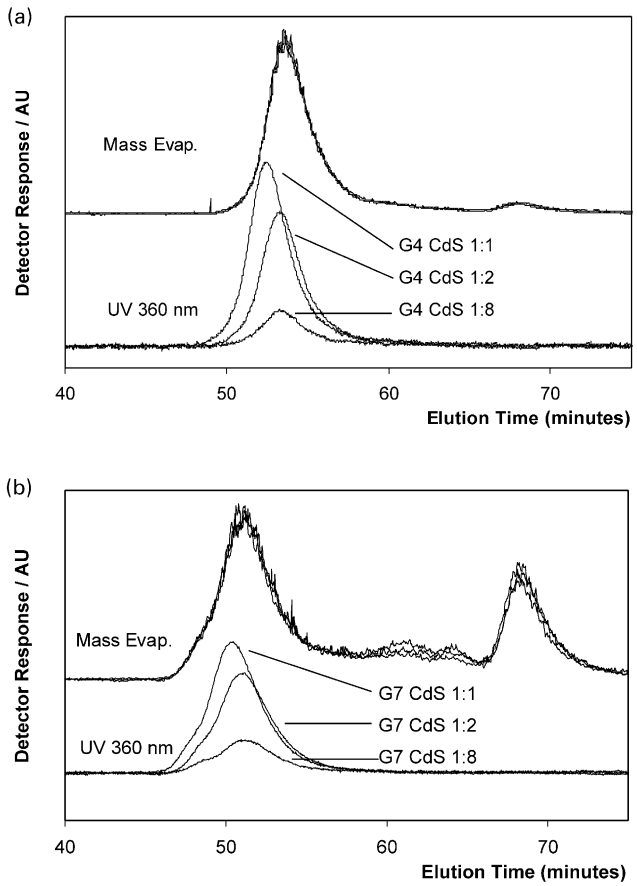

Fig. 4. Gel permeation chromatograph traces for (a) G4 CdS–stars and (b) G7 CdS–stars. Top: mass evaporative traces; bottom: ultraviolet absorbance detector traces at 360 nm.

change was seen in the mass evaporative detector trace as loading ratio increased to 1:1. (Development of a second peak at shorter elution time would suggest aggregate formation). It is possible that a small number of strongly absorbing aggregates are formed that are not seen by the mass evaporative detector due to a low mass fraction. Another possibility is that stars containing a larger CdS particle absorb more strongly at 360 nm. If these stars are also slightly larger and elute first, then the UV detector signal would shift towards shorter elution times.

3.6. Characterization of Au–stars by TEM

TEM was employed to observe the size distribution of Au particles. Fig. 5 shows images of G4, G7, and G10 Au–stars. Black dots correspond to gold particles; no polymer structure was visible. The number density of particles varied between photos because sample thickness was uncontrolled. Judging by the images, the Au particles were polydisperse. Particle sizes are estimated to be (<1–4) nm for G4 stars, (<1–6) nm for G7 stars, and (<1–3) nm for G10 stars. Average Au particle sizes were not calculated because the smallest particles (<1 nm) approach the resolution limit of the TEM. (For comparison, measured diameters of unmodified PAMAM–NH_2 dendrimers in good solvents are 4.6, 8.4, and 14.0 nm for G4, G7, and G10, respectively [31,32]). The Au particle size does appear to be related to dendrimer generation, although there is not a simple trend in particle size with increasing generation.

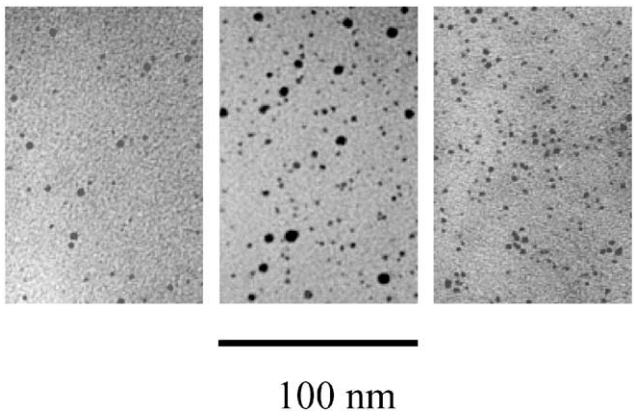

Fig. 5. Transmission electron microscope images for Au–stars. From left to right, G4 Au–stars, G7 Au–stars, G10 Au–stars.

Compared to unmodified PAMAM dendrimers, PAMAM/PEG stars control Au particle size in much the same way. G4 stars stabilized smaller Au particles compared to G7 stars, but the G10 stars produced the smallest Au particles. These observations are consistent with previous work on Au templating with PAMAM–NH_2 dendrimers [19]. The smaller Au particle size obtained with G10 dendrimers was previously attributed to the formation of multiple particles within each dendrimer rather than a single large particle. Although our TEM images cannot confirm multiple particles within the G10 stars, the apparent clustering of the gold particles on a 10–20 nm length scale and the small size of the Au particles support this assertion.

The TEM images of G4 Au–stars show Au particles randomly distributed throughout the samples. In these solid samples, no evidence of multiple Au particle aggregates was seen, even in lower magnification images. The outer shell of PEG may deter aggregate formation when the nanocomposites are isolated as solids. In contrast, previous TEM work on low generation (G2–G4) PAMAM–NH_2/Au nanocomposites in the solid state revealed aggregates consisting of tens or hundreds of Au particles and presumably dendrimers [10,19].

3.7. Characterization of CdS–stars by UV–vis and fluorescence spectroscopy

Our CdS–star samples could not be characterized by TEM because the technique was destructive towards the CdS particles. It was therefore necessary to infer CdS particle sizes from optical properties.

UV–vis absorption spectra (Fig. 6) were recorded for unmodified stars and CdS–stars. The absorption spectra of the unmodified stars exhibit a band near 280 nm due to the carbonyl groups in the dendrimer amides. CdS–star samples

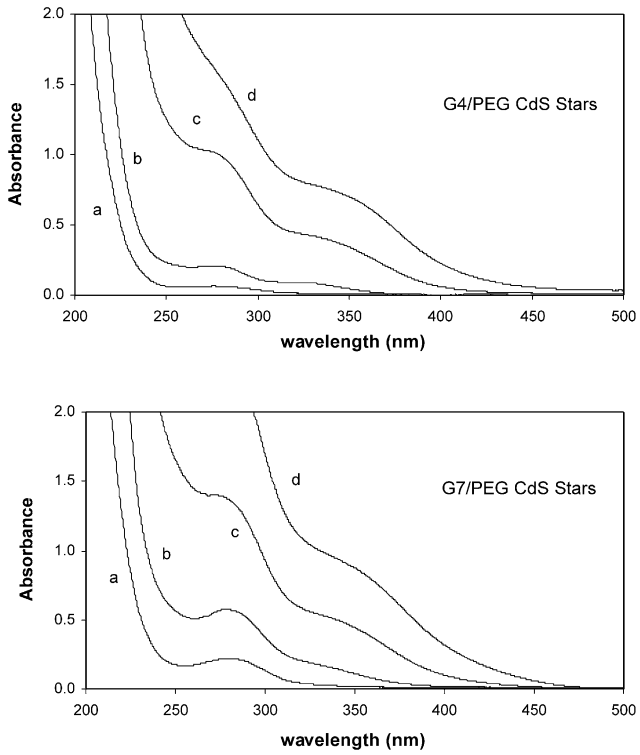

Fig. 6. UV–vis absorption spectra for G4 and G7 stars. Top: (a) unmodified G4 PAMAM/PEG stars; (b) G4 CdS 1:8; (c) G4 CdS 1:2; (d) G4 CdS 1:1. Bottom: (a) unmodified G7 PAMAM/PEG stars; (b) G7 CdS 1:8; (c) G7 CdS 1:2; (d) G7 CdS 1:1.

with loading ratios of 1:8 and 1:2 appeared colorless to the unaided eye, exhibiting the carbonyl absorption near 280 nm and a shoulder peak assigned to the CdS nanoparticles between 350 and 400 nm. Samples with loading ratio of 1:1 appeared yellow and have an absorption band edge above 400 nm, indicating the presence of comparatively larger CdS particles.

CdS particles with diameters less than about 6 nm are fluorescent due to the effects of quantum confinement on electronic structure, and exhibit optical properties dependent upon particle size and shape [33–36]. Fluorescence excitation and emission spectra were recorded for CdS–stars of varying dendrimer generation and loading ratio. Optical properties of samples are summarized in Table 2. Reported wavelengths corresponding to intensity maxima of excitation (λ_{ex}) and emission (λ_{em}) spectra have an estimated uncertainty of ± 5 nm. Excitation and emission spectra for the samples G4 CdS 1:8 and G4 CdS 1:1 are shown in Fig. 7 (curves a and b, respectively). Excitation and emission spectra for the samples G7 CdS 1:8 and G7 CdS 1:1 are shown in Fig. 8 (curves a and b, respectively). In Figs. 7 and 8, all intensities have been scaled by arbitrary constants to facilitate comparison of the lineshapes.

The CdS–star excitation spectra had features similar to the UV–vis absorption spectra, showing a global maximum typically between 350 and 400 nm and in some cases one or more shoulder peaks at shorter wavelengths. The slight differences between the spectra could be attributed to differences in particle size, shape, or surface structure. The excitation band edge moved to higher wavelength as loading ratio increased, in accordance with a growth in average particle size.

An estimate of particle size can be obtained from a published correlation [33] between UV absorbance and CdS particle diameter (as measured by small-angle X-ray scattering). Data from Ref. [33] (particle size vs. wavelength of UV absorbance threshold) indicate that an absorption threshold of 350 nm (3.54 eV) corresponds to a particle diameter of 2.0 nm, whereas a threshold of 435 nm (2.85 eV) corresponds to a diameter of about 3.0 nm. The absorption threshold of our CdS-loaded star samples is within that range, indicating that the average CdS particle diameters are approximately 2–3 nm. The absorption cutoff for the CdS–stars was not as sharp as that measured for monodisperse CdS nanoparticles [33], indicating that there is significant polydispersity in the size distribution. The estimate of 2–3 nm CdS particles is similar to the size of CdS particles found in previous studies using unmodified PAMAM dendrimers [7,8,11].

The fluorescence emission spectra of the CdS–star samples were rather broad (Figs. 7 and 8). For both G4 and G7 stars, the peak in emission intensity shifted to slightly higher wavelengths as loading ratio was increased (Table 2). Under a 365 nm light source, a progression of emission color from blue to yellow was observed as loading ratio was increased from 1:8 to 1:1. Although CdS nanoparticle emission spectra are affected by factors besides

Table 2
Optical properties of CdS-loaded star polymers (uncertainties quoted in text)

Sample name	Emission color[a]	Emission max.[b] λ_{em} (nm)	Excitation max.[c] λ_{ex} (nm)
G4 CdS 1:8	Indigo	464	342
G4 CdS 1:2	Blue	471	350
G4 CdS 1:1	Green	505	350
G7 CdS 1:8	Blue	465	341
G7 CdS 1:2	Green	502	353
G7 CdS 1:1	Yellow	521	362

[a] Appearance to the unaided eye under 365 nm irradiation.
[b] Wavelength corresponding to peak fluorescence intensity when irradiated at λ_{ex}.
[c] Wavelength corresponding to peak fluorescence intensity as observed at λ_{em}.

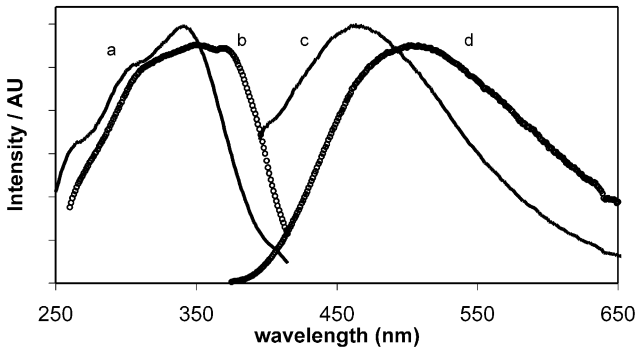

Fig. 7. Fluorescence spectra for G4 PAMAM/PEG CdS–stars. (a) G4 CdS 1:8 excitation spectrum; (b) G4 CdS 1:1 excitation spectrum; (c) G4 CdS 1:8 emission spectrum; (d) G4 CdS 1:1 emission spectrum.

particle size [33], this shift also supports an increase in the average CdS particle diameter with increasing loading ratio. It was not possible to obtain orange or red-emitting particles by further increasing the loading ratio. Rather, the solutions became increasingly yellow in normal light and emission color remained yellow. CdS optical properties may be changed by varying the loading ratio, but only to a certain extent.

The dendrimer generation affects CdS optical properties only weakly. Comparing samples with the same loading ratio, CdS particle sizes found for the G7 CdS stars are only slightly larger than those of the G4 CdS stars. Optical measurements therefore suggest that polymer structure exerts only limited control over CdS particle size under the reaction conditions employed. It is quite possible that the particle formation mechanism is not a simple templating reaction whereby the number of CdS molecules in a nanoparticle is determined by the dendrimer size. Rather, the characteristic size of the CdS nanoparticles may be in part determined by other factors such as solvent, temperature, and reactant mole ratios.

4. Conclusion

PAMAM/PEG dendrimer–star polymers retain the abilities of PAMAM dendrimers to template CdS or Au nanoparticles. According to GPC analysis, the size distribution of the stars is essentially unchanged by the addition of nanoparticles when the loading ratio is less than 1:1. Like PAMAM–NH_2 dendrimers, PAMAM/PEG stars typically stabilize polydisperse nanoparticles. However, modifying the PAMAM dendrimers with PEG has the desirable effect of improving miscibility with selected organic solvents and polymers. From a practical standpoint, the improvement in physical properties obtained by grafting PEG onto PAMAM endgroups could facilitate development and processing of novel nanocomposite materials.

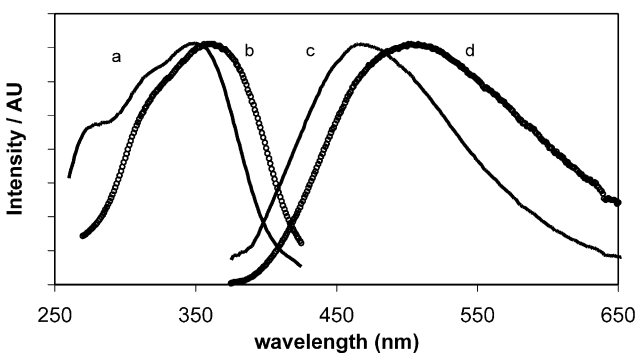

Fig. 8. Fluorescence spectra for G7 PAMAM/PEG CdS–stars. (a) G7 CdS 1:8 excitation spectrum; (b) G7 CdS 1:1 excitation spectrum; (c) G7 CdS 1:8 emission spectrum; (d) G7 CdS 1:1 emission spectrum.

Acknowledgments

Dr Hedden acknowledges the support of a National Research Council Research Associateship. We thank Dendritech, Inc. for providing the Generation 7 and 10 PAMAM dendrimers. The NIST Polymers Division staff is acknowledged for many helpful discussions.

References

[1] Tomalia DA, Baker H, Dewald J, Hall M, Kallos G, Martin S, Roeck J, Ryder J, Smith P. Polym J 1985;17:117–32.
[2] Crooks RM, Lemon BI, Sun L, Yeung LK, Zhao MQ. Top Curr Chem 2001;212:81–135.
[3] Zhao MQ, Sun L, Crooks RM. J Am Chem Soc 1998;120:4877–8.
[4] Balogh L, Tomalia DA. J Am Chem Soc 1998;120:7355–6.
[5] Ottaviani MF, Montalti F, Turro NJ, Tomalia DA. J Phys Chem B 1997;101:158–66.
[6] Hanus LH, Sooklal K, Murphy CJ, Ploehn HJ. Langmuir 2000;16: 2621–6.
[7] Lakowicz JR, Gryczynski I, Gryczynski Z, Murphy CJ. J Phys Chem B 1999;103:7613–20.
[8] Sooklal K, Hanus LH, Ploehn HJ, Murphy CJ. Adv Mater 1998; 10(14):1083–7.
[9] Huang J, Sooklal K, Murphy CJ. Chem Mater 1999;11:3595–601.
[10] Garcia ME, Baker L, Crooks RM. Anal Chem 1999;71:256–8.
[11] Lemon BI, Crooks RM. J Am Chem Soc 2000;122:12886–7.
[12] Zhao MQ, Crooks RM. Angew Chem Int Ed Engl 1999;38(3):364–6.
[13] Zhao MQ, Crooks RM. Chem Mater 1999;11:3379–85.
[14] Esumi K, Suzuki A, Yamahira A, Torigoe K. Langmuir 2000;16: 2604–8.
[15] Esumi K, Hosoya T, Suzuki A, Torigoe K. Langmuir 2000;16: 2978–80.
[16] Esumi K, Suzuki A, Aihara N, Usui K, Torigoe K. Langmuir 1998;14: 3157–9.
[17] Esumi K, Kameo A, Suzuki A, Torigoe K. Colloid Surf A 2001;189: 155–61.
[18] Gröhn F, Kim G, Bauer BJ, Amis EJ. Macromolecules 2001;34: 2179–85.
[19] Gröhn F, Bauer BJ, Akpalu Y, Jackson CL, Amis EJ. Macromolecules 2000;33:6042–50.
[20] Spanhel L, Haase M, Weller H, Henglein A. J Am Chem Soc 1987; 109:5649–55.
[21] Crooks RM, Zhao MQ, Sun L, Chechik V, Yeung LK. Acc Chem Res 2001;34(3):181–90.
[22] Zhao MQ, Crooks RM. Adv Mater 1999;11:217–20.
[23] Yeung LK, Crooks RM. Nanoletters 2001;1:14–17.

[24] Yeung LK, Lee CT, Johnston KP, Crooks RM. Chem Commun 2001; 21:2290–1.
[25] Niu YH, Yeung LK, Crooks RM. J Am Chem Soc 2001;123:6840–6.
[26] Viers B, Bauer BJ. Abstr Pap Am Chem Soc 2001;221:PMSE Part 2, 399–400.
[27] Miller JN. Standards in fluorescence spectrometry. London: Chapman & Hall; 1981.
[28] Velapoldi RA, Mielenz KD. A fluorescence standard reference material: quinine sulfate dihydrate. NBS/NIST Publication 260–64; 1980.
[29] Hedden RC. Unpublished results.
[30] Chechik V, Zhao MQ, Crooks RM. J Am Chem Soc 1999;121: 4910–1.
[31] Topp A, Bauer BJ, Tomalia DA, Amis E. Macromolecules 1999;32: 7232–7.
[32] Prosa TJ, Bauer BJ, Amis EJ. Macromolecules 2001;34:4879–906.
[33] Vossmeyer T, Katsikas L, Giersig M, Popovic IG, Diesner K, Chemseddine A, Eychmüller A, Weller H. J Phys Chem 1994;98: 7665–73.
[34] Eychmüller A. J Phys Chem B 2000;104:6514–28.
[35] Weller H. Angew Chem Int Ed Engl 1993;32:41–53.
[36] Murray CB, Norris DJ, Bawendi MG. J Am Chem Soc 1993;115: 8706–15.